Contents lists available at SciOpen

Food Science and Human Wellness

journal homepage: https://www.sciopen.com/journal/2097-0765

China Food Publishing Co.

Cytisine *N*-methylene-(5,7,4′-trihydroxy)-isoflavone induces neural stem cell proliferation and reverses cognitive deficits in early Alzheimer's disease models *via* canonical Wnt/*β*-catenin pathway

Yangyang Lu[a,†], Xiaowan Li[b,†], Zhiping Qin[a], Wenjing Sun[a], Yongbiao Li[a], Shaobo Liu[a], Lu Lu[a], Rongfei Yang[a], Nana Zhang[a], Yiting Liu[a], Jun Zhang[c,*], Qingshan Liu[a,*]

[a] *Key Laboratory of Ethnomedicine for Ministry of Education, Center on Translational Neuroscience, Minzu University of China, Beijing 100081, China*
[b] *Center for Life Sciences, School of Life Science and Technology, Harbin Institute of Technology, Harbin 150001, China*
[c] *Department of Ophthalmology, Shandong Provincial Hospital Affiliated to Shandong First Medical University, Jinan 250021, China*

ARTICLE INFO

Article history:
Received 21 November 2023
Received in revised form 2 April 2024
Accepted 24 April 2024

Keywords:
Alzheimer's disease
5×FAD mice
Neural stem cells
Isoflavone-cytisine
Wnt/*β*-catenin

ABSTRACT

Alzheimer's disease (AD) is a degenerative disease of the central nervous system. It results in cognitive dysfunction due to the loss of functional neurons and a deficit of new neurons, which can lead to death in severe cases. Repairing damaged neurons by promoting hippocampal neurogenesis has become therapeutic modality to combat neurodegenerative diseases. The novel isoflavone alkaloid LY01, found in the edible fruits of *Sophora alopecuroides* L., has various neuroprotective effects. However, the molecular mechanism by which it promotes the proliferation of endogenous neural stem cells (NSCs) is not yet precisely known. The effects of LY01 were investigated *in vivo* and *in vitro*. *In vivo* experiments showed that LY01 could counteract the toxic damage of amyloid β-protein (Aβ), enhance the learning ability and memory capacity of 5×FAD mice, and improve the morphology of neurons in the hippocampal region. *In vitro* experiments showed that LY01 was effective against antioxidant damage, improved the cell morphology of C17.2 mouse NSCs after hydrogen peroxide injury, and increased cell viability. Both *in vitro* and *in vivo* experiments promoted NSC proliferation by upregulating the mRNA and protein levels of the critical genes of the Wnt/*β*-catenin pathway, which increased levels of doublecortin to facilitate new neuronal generation. This indicates that the ability of LY01 to counteract Aβ toxicity and alleviate oxidative damage in early AD is associated with activation of the Wnt/*β*-catenin signaling pathway to promote NSC proliferation and thus repair damaged neurons.

1. Introduction

Alzheimer's disease (AD) is pathologically characterized by massive neurofibrillary tangles formed by tau protein hyperphosphorylation and senile plaques formed by *β*-amyloid deposition causing extensive degeneration and loss of neurons in the hippocampus of the brain. Its main clinical manifestations are cognitive dysfunction and memory impairment due to the loss of functional neurons and the absence of new neurons; it is currently incurable[1-2]. Damaged neurons can be repaired by stem cell transplantation promoting the proliferation of neural stem cells (NSCs)[3-4], which have a limited regenerative capacity even after the brain has matured, offering the possibility of brain injury repair. Endogenous NSCs can be "recruited" to lesioned or damaged areas of the brain to participate in neural regeneration and

† These authors have contributed equally to this work.
* Corresponding authors.
E-mail address: slhlzj2024@163.com (J. Zhang); nlqsh@163.com (Q.S. Liu)
Peer review under responsibility of Beijing Academy of Food Sciences.

SciOpen Publishing services by Tsinghua University Press

http://doi.org/10.26599/FSHW.2024.9250259

repair. However, the feedback from the body caused by external injury stimuli alone is still insufficient to enable the limited number of NSCs in the body to achieve neural self-repair and functional reconstitution[5-6]. Therefore, how to promote the proliferation of NSCs through exogenous induction needs to be further explored.

Sophora alopecuroides L., genus *Sophora* of the subfamily Papilionoideae, family Leguminosae, is a plant mainly distributed in the desert and semi-desert areas of northwest China and Western and Central Asia. People in Northern China use the fruits and seeds in their diet, mixing them with wheat flour. Cytisine *N*-methylene-(5,7,4′-trihydroxy)-isoflavone (LY01, Fig. 1A) has been found in the fruits of *S. alopecuroides* L. and has neuroprotective effects. Neurodegenerative diseases result in the progressive loss or death of neuronal structure or function, leading to functional impairment. These include Parkinson's disease and AD, among others, and pose a severe threat to human health and daily life[7]. Studies suggest that LY01 has neuroprotective effects against degenerative lesions, promotes neural regeneration in AD[8], and alleviates neuroinflammation in Parkinson's disease[9], but its molecular mechanism remains unclear. The etiology of AD is complex, and its pathogenesis is unclear. The main etiological hypotheses include the amyloid β-protein (Aβ) toxicity hypothesis, the tau protein hypothesis, the inflammation hypothesis, and the oxidative damage hypothesis[1,10-13]. Therefore, we explored the effects of LY01 on the proliferation of NSCs under different damage, as well as its molecular mechanisms, using *in vivo* (Fig. 1B) and *in vitro* (Fig. 1C) experiments.

2. Materials and methods

2.1 Animal grouping

The 5×FAD transgenic mice were APP/PS1 transgenic AD models carrying 5 familial mutations. Intracellular Aβ-42 accumulation in neuronal cells can be observed in this strain of mice from 1.5 months of age, recapitulating the main features of β-amyloid deposition pathology in AD[14]. Two-month-old male 5×FAD mice (Beijing Institute of Basic Medical Sciences, Beijing, China) were housed in a constant-temperature ((23.0 ± 2.0) °C) and constant humidity (40%–60%) rearing room with a 12-h light/dark cycle and acclimatized feeding for 1 week. The experiments were approved by the Animal Protection and Utilization Committee of the Minzu University of Nationalities (approval number: ECMUC2021012AA). All experimental animal procedures were performed following the Guide for the Care and Use of Laboratory Animals (NIH Publication, 1999 Revision, No. 3040-2, Bethesda, MD, USA). The experiments were divided into 6 groups of 8 per group. Except for the wild-type (WT) group, all groups were 5×FAD mice. The WT and model groups were injected with equal amounts of saline daily. The masculine drug was ginsenoside Rg1, the main active monomer compound from the Chinese herb ginseng, which has significantly improved cognitive impairment in AD animals[15-17]. The Rg1 group was administered at a dose of 20 mg/(kg·day), and the low, medium, and high doses of LY01 were 25, 100, and 400 μg/(kg·day), by intraperitoneal injection once a day for 5 weeks. Behavioral tests were performed on the mice at week 4. Mice were injected with bromodeoxyuridine (BrdU) at a dose of 50 mg/(kg·day) daily for three consecutive days starting 4 days before sacrifice. After 5 weeks, they were anesthetized with 10% chloral hydrate and perfused with saline for cardiac perfusion, and intact brain tissue was removed. The right hemi-brains of each group were fixed in 4% paraformaldehyde, and the left hemi-brains of each group were stored at −80 °C.

2.2 Morris water maze (MWM) test

The MWM is a classic method used to test experimental animals' spatial learning ability and memory capacity[18-19]. The water maze experimental apparatus (Chengdu Taimeng, WMT-100, China) was a pool of water divided into four quadrants, and a quadrant was chosen to set up an escape platform for mice to stand and remain in the same position. Water was added to the pool, the escape platform was covered by 2 cm, and the water temperature was kept at 22 °C. Milk was added to make the water surface turbid. The training experiment was designed for 6 days, with each mouse entering the water from each of the 4 quadrants, and the experiment was stopped each time it found a platform in the water within 60 s. The process used is referred to as the latency period. If the mouse did not find the platform within the specified time, it was guided to the platform and stayed there for 10 s to deepen learning. On day 7, the platform was removed, and the mice were placed in the water from the opposite quadrant of the platform. The number of times they crossed the platform, the swimming distance, and the change in dwell time within 60 s were recorded[20].

2.3 Hematoxylin-eosin (HE) staining

HE staining was performed by paraffin sectioning. Three right hemi-brains fixed in 4% paraformaldehyde for 24 h were removed from each group, dehydrated with sucrose gradient, and fixed with paraffin, and the classical hippocampal region tissue was cut at a thickness of 5 μm. After dewaxing, the sections were stained with a hematoxylin staining solution for 5 min and then washed with distilled water and fractionated in 1% hydrochloric acid for 30 s. After the sections turned red, differentiation was stopped rapidly with distilled water. The eosin staining solution was re-stained for 15 s. After

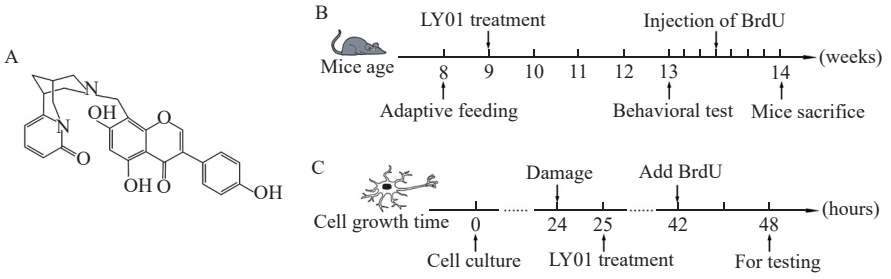

Fig. 1 (A) Chemical structure of LY01. (B) Schedule for animal experiment. (C) Schedule for cellular experiments.

dehydration and sealing, the sections were photographed under a microscope to observe the pathological condition of the classic hippocampal region of brain tissue[21-22].

2.4 Cell grouping

The C17.2 mouse NSC line was an immortalized one[23]. C17.2 mouse NSCs (Tianjin Saierbio, China) were cultured in a cell culture incubator (Thermo Fisher, HERA cell 150, USA) at 37 ℃, 95% O_2, 5% CO_2 for 24 h. All groups except the normal group were molded with 100 μmol/L hydrogen peroxide for 30 min and then switched to a drug-containing Dulbecco's modified Eagle's medium (DMEM) for 24 h. The experiment was divided into 6 groups: the normal group was maintained in normal DMEM without molding, the model group was maintained in standard DMEM after molding, the positive drug group was maintained in DMEM containing ginsenoside Rg1 (25 μmol/L after molding), and the LY01 high/middle/low-dose groups were maintained in DMEM containing LY01 (25, 12.5, 6.25 μmol/L) after molding. Cells were added to BrdU at a concentration of 30 μmol/L for 6 h at hour 42, then used for BrdU staining. Cell morphology was observed (Olympus, TE16721, Japan), and cell viability was determined after 48 h.

2.5 Cell viability assay

Cell counting kit-8 (CCK-8; Solarbio, CK04, China) is a highly sensitive colorimetric assay that can determine cell proliferation activity. Treatments were performed with 96-well plates (density 2×10^5 cells/mL). The old medium was aspirated, and 90 μL of medium and 10 μL of CCK-8 solution were added to each well and incubated for 1.5 h at 37 ℃ after 48 h. The optical density (OD) value of each well was measured at 450 nm on an enzyme-linked immunoassay (Molecular Devices, Flex Station 3, USA). Cell viability was calculated as follows:

Cell viability (%) = (OD value of experimental group − OD value of blank group)/(OD value of control group − OD value of blank group) × 100

2.6 Immunofluorescence assay

Brain tissue immunofluorescence was performed using frozen sections. Four right hemi-brains fixed with 4% paraformaldehyde were removed from each group, dehydrated with sucrose gradient, fixed with an embedding agent, and frozen, and the classical hippocampal region tissue was cut at a thickness of 30 μm. The tissues were closed with phosphate buffered saline (PBS) containing 1% bovine serum albumin (BSA), 10% goat serum, and 0.3% triton at room temperature for 1 h. Nestin primary antibody (Abcam, USA, ab81462) was diluted at 1:500, BrdU primary antibody (Cell Signaling Technology, UK, 5292S) at 1:400, and doublecortin (DCX) primary antibody (Cell Signaling Technology, UK, 14802S) at 1:1 000 with enhanced antibody diluent (Abbkine, USA, BMU103-CN; Cell Signaling Technology, 14802S). These were incubated overnight at 4 ℃. Secondary antibody (Abbkine, A23240, USA) was added to 1% BSA and 0.3% triton in PBS at 1:400 and incubated for 90 min at room temperature, avoiding light. Three washes with PBS were required after each step. A drop of DAPI (Solarbio, C0065, China) was added and then incubated for 5 min at room temperature, avoiding light. A drop of anti-fluorescence decay blocker (Solarbio, S2100, China) was added, and the film was sealed.

Cellular immunofluorescence was performed using cell crawl sheets. Cells were fixed with 4% paraformaldehyde for 30 min at room temperature. BrdU staining required acidification with 2 mol/L hydrochloric acid for 1 h[24]. Cells were punched by adding PBS containing 0.5% triton X-100 prepared at room temperature for 20 min. Closure was performed with PBS containing 10% goat serum for 1 h at room temperature. Nestin primary antibody (Abcam, ab81462, UK) was diluted at 1:200. BrdU primary antibody (Cell Signaling Technology, USA, 5292S) was diluted at 1∶400 with PBS containing 5% goat serum. The cell crawls were incubated upside down on a flat sealing film at 4 °C overnight. The secondary antibody (Abbkine, A23240, USA) was diluted with PBS at 1:1 000 and incubated for 1 h at room temperature, avoiding light. Three washes with PBS were required after each step. A drop of DAPI was added before incubating for 5 min at room temperature. A drop of anti-fluorescence attenuation blocker was added, and the slice was sealed.

A laser confocal microscope (Leica, TCS SP8, Germany) was used for observation, and the excitation light and voltage were adjusted according to the situation to make the images clear for photo preservation. Images were used in ImageJ software to analyze particles.

2.7 Real-time fluorescence quantitative polymerase chain reaction (qPCR)

Four left hemi-brains from each group stored at −80 °C were used to extract total RNA from hippocampal tissue. Cells cultured in 6-well plates were used to extract total cellular RNA. Total RNA was isolated using a TRIzol reagent and analyzed by purity and concentration. The cDNA was synthesized by GenStar reverse transcription kit (Genstar, A224-10, China). Real-time fluorescence qPCR was performed by 2× RealStar Fast SYBR qPCR Mix (Genstar, A301-10, China) and LightCycler® 96 real-time PCR detection system (Roche, Basel, Switzerland) instruments under cycling conditions: 95 ℃ for 2 min, followed by 45 cycles of 95 ℃ for 15 s and 60 ℃ for 15 s. The primer sequences are shown in Table 1. The $2^{-\Delta\Delta Ct}$ method was used to quantify the mRNA levels of the genes[25].

Table 1
Primers sequences for qPCR.

Genes	Sequences of primers (5′-3′)
GAPDH	Forward: CATCACTGCCACCCAGAAGACTG
	Reverse: ATGCCAGTGAGCTTCCCGTTCAG
β-catenin	Forward: GTTCGCCTTCATTATGGACTGCC
	Reverse: ATAGCACCCTGTTCCCGCAAAG
Wnt3a	Forward: AACTGCACCACCGTCAGCAACA
	Reverse: AGCGTGTCACTGCGAAAGCTAC
cyclinD1	Forward: GCAGAAGGAGATTGTGCCATCC
	Reverse: AGGAAGCGGTCCAGGTAGTTCA
GSK-3β	Forward: GAGCCACTGATTACACGTCCAG
	Reverse: CCAACTGATCCACACCACTGTC

2.8 Western blot (WB)

Four left hemi-brains from each group stored at −80 ℃ were used to extract total protein from hippocampal tissue. Cells cultured in 6-well plates were used to extract total cellular protein. Total protein was extracted using radioimmunoprecipitation assay (RIPA) lysis buffer (Beyotime, P0013B, China) containing 1% phenylmethanesulfonyl fluoride. Protein concentration was determined using the BCA protein quantification kit (Beyotime, P0010s, China). Proteins were separated by 10% sodium dodecyl sulfate-polyacrylamide gel electrophoresis and transferred to PVDF membranes. After sealing with 5% skimmed milk powder for 1 h, the membranes were mixed with different primary antibodies: anti-β-actin (Cell Signaling Technology, 4970s, USA), anti-Wnt3a (Abcam, ab28472, UK), anti-β-catenin (Cell Signaling Technology, 9562S, USA), and anti-cyclinD1 (Abcam, ab40754, UK). They were incubated overnight at 4 ℃. The membranes were rinsed with tris-buffered saline with tween 20 (TBST) buffer and incubated in the corresponding secondary antibody (ZSGB-BIO, ZB-2306, China) for 2 h. The antibody dilution ratio was 1∶1 000; anti-cyclinD1 was diluted with TBST containing 5% BSA, and other antibodies were diluted with 5% skimmed milk powder. PVDF membranes were observed by enhanced chemiluminescence (Beyotime, P0018AS, China) and photographed using a Tanon chemiluminescence imager (Tanon, Tanon 4200, China). The intensity of each band for different samples was measured using ImageJ software and normalized to the level of the internal reference β-actin[26].

2.9 Statistical analysis

All statistical analyses were performed using GraphPad Prism version 8.0 software. The normality test (D'Agostino-Pearson omnibus test) and chi-square test (Brown-Forsythe test) were performed first. One-way analysis of variance was used for data that conformed to the normal distribution and chi-square, and the non-parametric test was used for those that did not. Data were expressed as mean ± standard deviation (SD). The threshold of significance was set at $^{*}P < 0.05$, $^{**}P < 0.01$, $^{***}P < 0.001$.

3. Results

3.1 LY01 improves cognitive deficits in 5×FAD mice

The water maze evaluated the mice's spatial learning ability and memory capacity. Learning ability was assessed by escape latency and swimming distance, and memory capacity was expressed as the number of times crossing the platform and the proportion of time spent in the target quadrant[18]. The motor trajectory diagram (Fig. 2A) demonstrates that the mice in the 5×FAD group showed disorganized motor trajectories, whereas the WT, Rg1, and LY01 groups administered at each dose showed motor trajectories enriched in the target quadrant. The latency to escape (Fig. 2B) of each group decreased with the increased number of training sessions, indicating that the training was practical. In each training experiment, the latency period of 5×FAD mice was greater than that of the WT group ($P < 0.05$), indicating that 5×FAD mice had learning disabilities. The latency periods of mice in the Rg1 and LY01 medium-and high-dose groups were shorter than those in the 5×FAD group on the 5th day of the experiment ($P < 0.05$). The latency periods of mice in the Rg1 and LY01 medium- and high-dose groups were shorter than those in the 5×FAD group on the sixth day of the experiment ($P < 0.001$). This indicates that Rg1 and LY01 significantly improved the learning ability of 5×FAD mice. The swimming distance of mice reaching the platform for the first time in the experiment (Fig. 2C) was greater for 5×FAD mice than the WT group ($P < 0.05$), indicating that 5×FAD mice had learning disabilities. The swimming distance of mice in the Rg1 group ($P < 0.05$) and LY01 medium- and high-dose groups ($P < 0.001$) was shorter than that of the 5×FAD group, indicating that Rg1 and LY01 significantly improved the learning ability of 5×FAD mice. The results for the number of times the mice crossed the platform (Fig. 2D) and the time they stayed in the target quadrant (Fig. 2E) on day 7 showed that the 5×FAD mice crossed the platform less often than the WT group ($P < 0.01$) and the 5×FAD mice stayed in the target quadrant for less time than the WT group ($P < 0.05$), indicating that the 5×FAD mice had memory impairment. In contrast, the number crossing the platform was higher in the Rg1 and LY01 medium-dose groups than in the 5×FAD mice ($P < 0.05$). The number of platform crossings trended higher in the LY01 low- and high-dose administration groups than in the 5×FAD mice, as well as in the target quadrant in the Rg1 group and each dose administration group of LY01 indicating that Rg1 and LY01 can improve the memory ability of the 5×FAD mice.

3.2 LY01 improves neural cell morphology in the hippocampus

In HE staining, the hematoxylin stain is primary and stains the chromatin in the nucleus and nucleic acids in the cytoplasm, mainly violet-blue. Eosin is an acidic dye that stains the cytoplasm and extracellular matrix components, primarily violet-red. HE staining enables clear visualization of cell and tissue morphology[27]. The normal cell morphology in the hippocampal region is round and neatly arranged, with the cytoplasm stained violet-red over a large area and the chromatin in the nucleus and nucleic acids in the cytoplasm stained violet-blue in only a small area. The abnormal cells in the hippocampal region were irregular in morphology and abnormally closely arranged, and the whole cells were stained violet-blue. The HE staining results of the cornu ammonis (CA)2, CA3, and the dentate gyrus (DG) regions of the hippocampus showed that the cell morphology of the CA2, CA3, and DG regions of the hippocampus in the WT group was round and neatly arranged (Fig. 3B). Hippocampal subdivisions were showed in Fig. 3A. In contrast, the CA2, CA3, and DG regions of the hippocampus in the 5×FAD group were deeply stained violet-blue with irregular cell shapes. This indicates the specific potential of Rg1 and LY01 to improve the abnormal morphological cells in the hippocampal region of mice caused by Aβ deposition.

3.3 LY01 promotes the proliferation of NSCs in the hippocampus

Immunofluorescence is a technique for antigen localization that labels antibodies with fluorescent substances. The proliferation of NSCs was determined by labeling the NSCs cytoskeleton protein nestin, as well as BrdU that substitutes for thymine (T) infiltration, into the DNA synthesis (S) phase: replicating[28]. Figs. 4A and B show the hippocampal DG region nestin and BrdU, respectively. Hippocampal DG region showed in Fig. 4C. The proportion of positive cells in the DG region of the hippocampus (Figs. 4D-E) showed that the nestin and BrdU

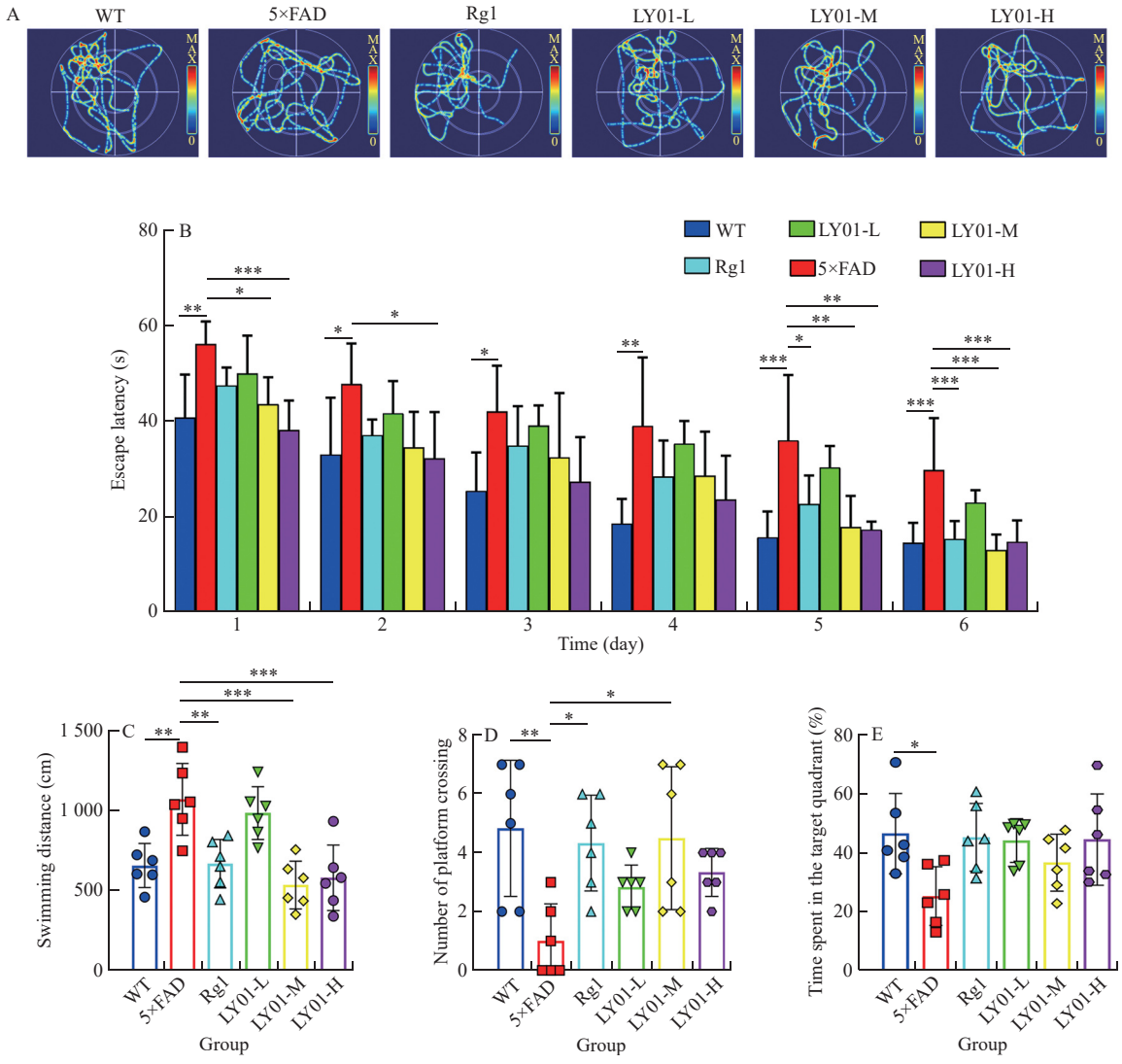

Fig. 2 LY01 improves cognitive deficits in 5×FAD mice. (A) Heat map of swimming path in MWM test. (B) Escape latency in the training trials. (C) Swimming distance before the first crossing of the platform. (D) The number of crossings of the target quadrant. (E) Time spent in the target quadrant. $^{*}P < 0.05$, $^{**}P < 0.01$, $^{***}P < 0.001$,the same as below. $n = 6$. LY01-L = 25 μg/(kg·day), LY01-M = 100 μg/(kg·day), LY01-H = 400 μg/(kg·day). Same with Figs. 3-6.

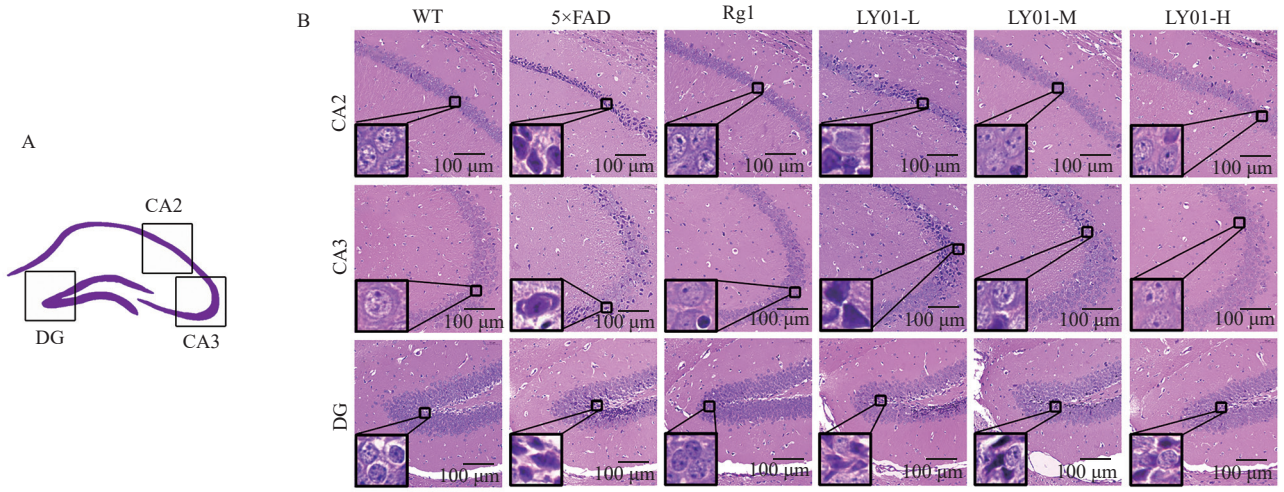

Fig. 3 LY01 improves neural cell morphology in the hippocampus. (A) Location and partitioning of hippocampal sections for HE staining. (B) Results of HE staining in the hippocampus's CA2, CA3, and DG regions. A normal cell is round and neatly arranged, with the cytoplasm stained violet-red over a large area and the chromatin in the nucleus and nucleic acids in the cytoplasm stained violet-blue only in a small area. Abnormal cells are irregular in morphology and abnormally closely arranged; the whole cells were stained violet-blue.

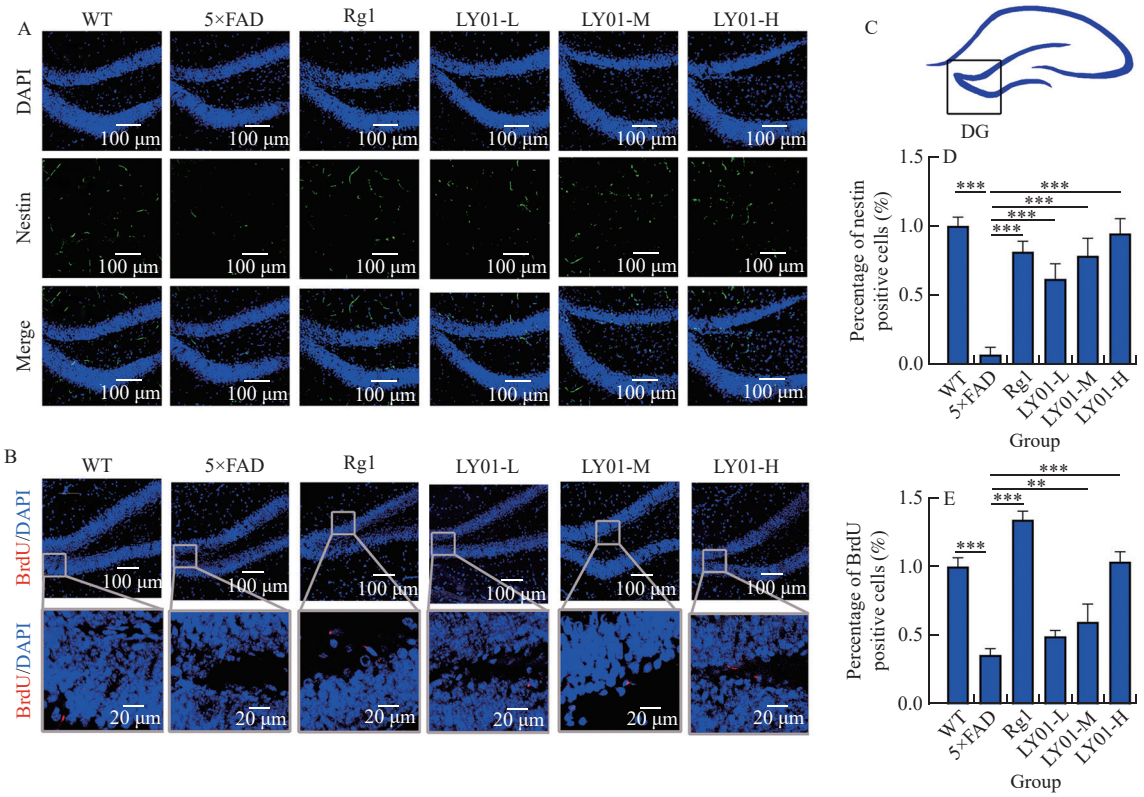

Fig. 4 LY01 promotes the proliferation of NSCs in the hippocampus. (A) Nestin immunofluorescence staining results in the DG region of the hippocampus. (B) BrdU immunofluorescence staining results in the DG region of the hippocampus. (C) Location and partition of hippocampal sections used for immunofluorescence. (D) Percentage of nestin-positive cells. (E) Percentage of BrdU positive cells. $n = 4$.

content in the 5×FAD group was much lower in the WT group ($P < 0.001$). This indicated that Aβ deposition inhibited the proliferation of NSCs. However, the nestin and BrdU content in each dose group of Rg1 and LY01 was much higher than that in the 5×FAD group ($P < 0.001$) but lower than in the WT group. This indicated that the Rg1 and LY01 dose groups could significantly counteract the inhibitory effect of Aβ deposition on the proliferation of NSCs in the DG region of the hippocampus and act as a pro-proliferative agent.

3.4 LY01 promotes new neuronal generation in the hippocampus

Transiently expressed DCX was used to label neonatal neurons[3]. Fig. 5A demonstrates the DCX in the DG area of the hippocampus. Hippocampal DG region showed in Fig. 5B. The proportion of positive cells in the DG region of the hippocampus (Fig. 5C) showed that the DCX content in the 5×FAD group was much lower than in the WT group ($P < 0.001$). This indicated that Aβ deposition inhibited neuronal production. In comparison, the content of DCX in each dose group of

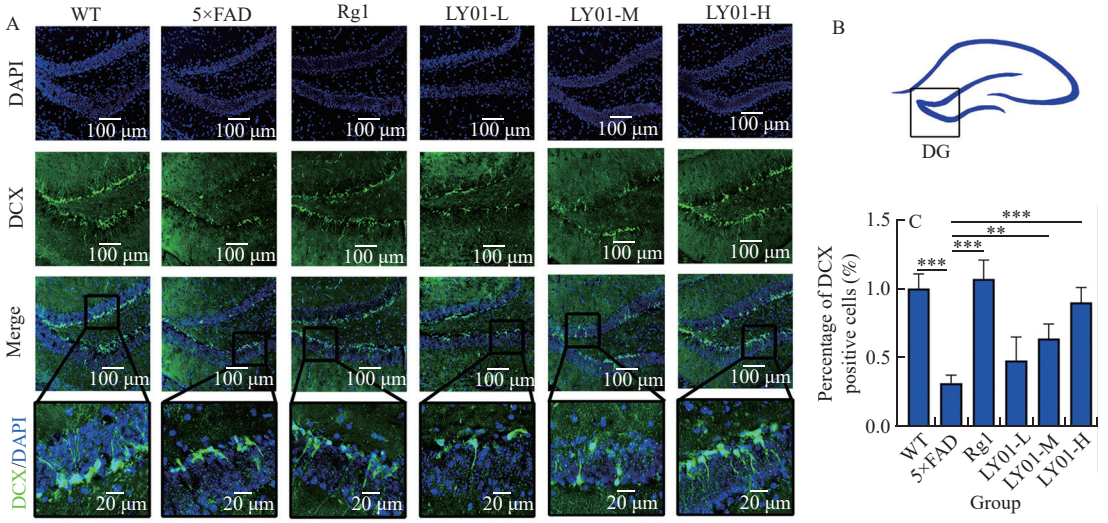

Fig. 5 LY01 promotes new neuronal generation in the hippocampus. (A) DCX immunofluorescence staining results in the DG region of the hippocampus. (B) Location and partition of hippocampal sections used for immunofluorescence. (C) Percentage of DCX positive cells. $n = 4$.

Rg1 and LY01 was much higher than that in the 5×FAD group ($P < 0.001$) but lower than that in the WT group. This indicated that each dose administration group of Rg1 and LY01 can significantly counteract the inhibitory effect of Aβ deposition on the generation of new neurons in the DG region of the hippocampus, which is beneficial to the generation of new neurons.

3.5 LY01 has the potential to activate the Wnt/β-catenin signaling pathway in the hippocampus

Adult hippocampal neurogenesis is associated with cognitive function. Neurogenesis involves a multistep process of generating new neurons through fine-tuning, such as proliferation, migration, and differentiation of NSCs[29]. At the same time, the activation of the Wnt/β-catenin signaling pathway promotes hippocampal neurogenesis[30-32]. qPCR and WB detected critical factors in the Wnt/β-catenin signaling pathway. The qPCR results showed that the mRNA expressions of *Wnt3a* (Fig. 6A), *β-catenin* (Fig. 6C), and *cyclinD1* (Fig. 6D) in the 5×FAD group were lower than those in the WT group (*Wnt3a*: $P = 0.599\,8$, *β-catenin*: $P < 0.05$, *cyclinD1*: $P < 0.001$). The mRNA expression of *GSK-3β* in the 5×FAD group (Fig. 6B) was higher than that in the WT group ($P < 0.001$), indicating that Aβ deposition promotes *GSK-3β* phosphorylation, reduces the production of *Wnt3a*, *β-catenin*, and *cyclinD1*; and inhibits the Wnt/β-catenin signaling pathway. In contrast, the mRNA expression of *Wnt3a* (Fig. 6A), *β-catenin* (Fig. 6C), and *cyclinD1* (Fig. 6D) was significantly higher ($P < 0.05$) and *GSK-3β* was substantially lower ($P < 0.05$) in the Rg1 and LY01 groups administered at each dose than in the 5×FAD group. This indicated that the Rg1 and LY01 groups administered the drug groups at each dose had the potential to activate the Wnt/β-catenin signaling pathway in the hippocampus.

The WB results showed that the protein expression of Wnt3a (Fig. 6G), β-catenin (Fig. 6F), and cyclinD1 (Fig. 6H) in the 5×FAD group was lower than that in the WT group (Wnt3a: $P < 0.01$, β-catenin: $P < 0.001$, cyclinD1: $P < 0.001$). This indicated that Aβ deposition decreases Wnt3a, β-catenin, and cyclinD1 production and inhibits the Wnt/β-catenin signaling pathway. In comparison, the protein expression of Wnt3a (Fig. 6G), β-catenin (Fig. 6F), and cyclinD1 (Fig. 6H) was significantly higher in the Rg1 and LY01 administration groups at each dose than in the 5×FAD group ($P < 0.05$). This indicated that the Rg1 and LY01 groups administered at each dose had the potential to activate the Wnt/β-catenin signaling pathway in the hippocampus.

3.6 LY01 increases the cell viability of C17.2 mouse NSCs

The immunofluorescence identification of nestin showed that NSCs were the cell line used (Fig. 7B). At 48 h, the cell morphology results revealed a stark contrast between the normal and model groups (Fig. 7A). The normal group exhibited spread cell morphology with orderly growth against the wall. In contrast, the model group displayed crinkled cell morphology with floating dead cells. However, the Rg1 and LY01 dose groups improved cell death and crinkled cell morphology due to oxidative damage, with only a few cells in suspension. The cell viability (Fig. 7C) and cell count[30] (Fig. 7D) results further confirmed the detrimental effects of oxidative damage, with significantly lower cell viability and number in the model group compared to the normal group ($P < 0.001$). Significantly, the Rg1 and LY01 dose administration groups demonstrated marked improvement in cell viability and number compared to the model group ($P < 0.001$). Although they had not yet reached normal levels, these results underscore the potential of Rg1 and LY01 in enhancing cell viability in response to antioxidant injury.

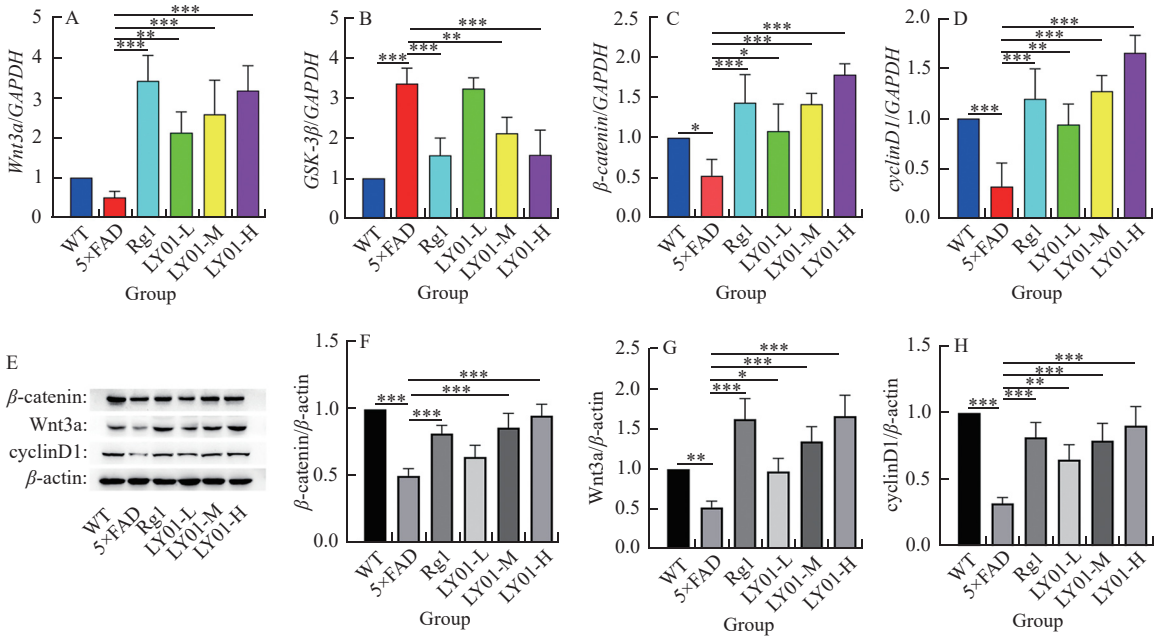

Fig. 6 LY01 promotes activation of the Wnt/β-catenin signaling pathway in the hippocampus. (A) Relative mRNA expression of *Wnt3a*. (B) Relative mRNA expression of *GSK-3β*. (C) Relative mRNA expression of *β-catenin*. (D) Relative mRNA expression of *cyclinD1*. (E) Protein expression of β-catenin, Wnt3a, cyclinD1. (F) Relative protein expression of β-catenin. (G) Relative protein expression of Wnt3a. (H) Relative protein expression of cyclinD1. $n = 4$.

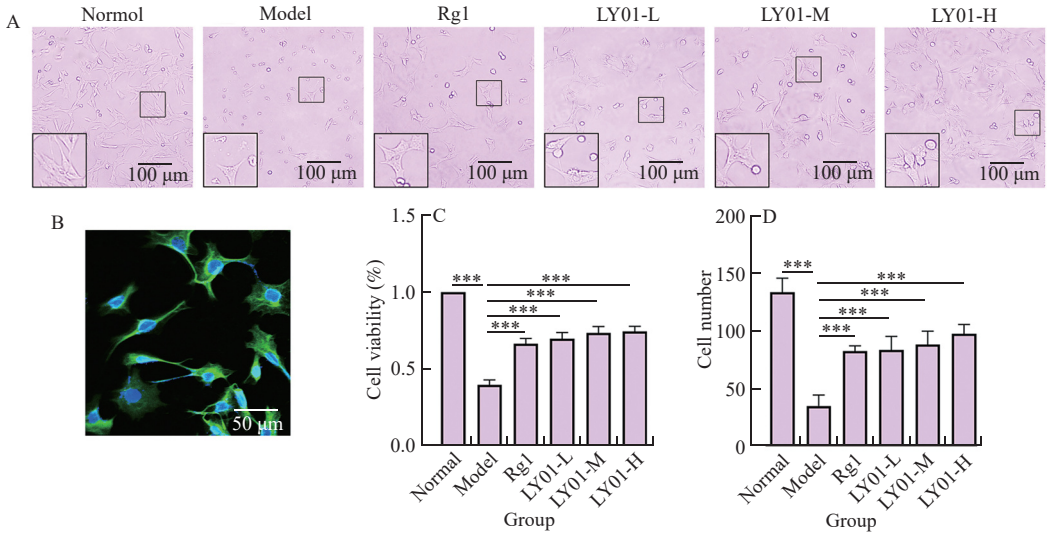

Fig. 7 LY01 increases the cell viability of C17.2 mouse NSCs. (A) Cell morphology after 48 h of cultivation. (B) Identification of C17.2 mouse NSCs using nestin immunofluorescence. (C) Cell viability. (D) Cell counting in the field of view of cell morphology observation. $n = 3$. LY01-L = 6.25 μmol/L, LY01-M = 12.5 μmol/L, LY01-H = 25 μmol/L. Same with Figs. 8 and 9.

3.7 LY01 promotes proliferation of C17.2 mouse NSCs

The nestin immunofluorescence results (Fig. 8A) and BrdU immunofluorescence results (Fig. 8C) showed that the normal group had dense cells with a spreading morphology. The model group had sparse cell numbers and wrinkled morphology. Compared with the model group, the cell density increased, and the cell morphology was normal in the Rg1 and LY01 administration groups at each dose. The results of the nestin-positive cell (Fig. 8B) and BrdU-positive cell counts (Fig. 8D) showed that the cell numbers in the model group were significantly lower than those in the normal group ($P < 0.001$). In contrast, the cell numbers in the Rg1 and LY01 dose administration groups were considerably higher than those in the model group ($P < 0.001$). However, they did not return to normal levels, suggesting that the Rg1 and LY01 dose administration groups can potentially promote the proliferation of NSCs in response to antioxidant injury.

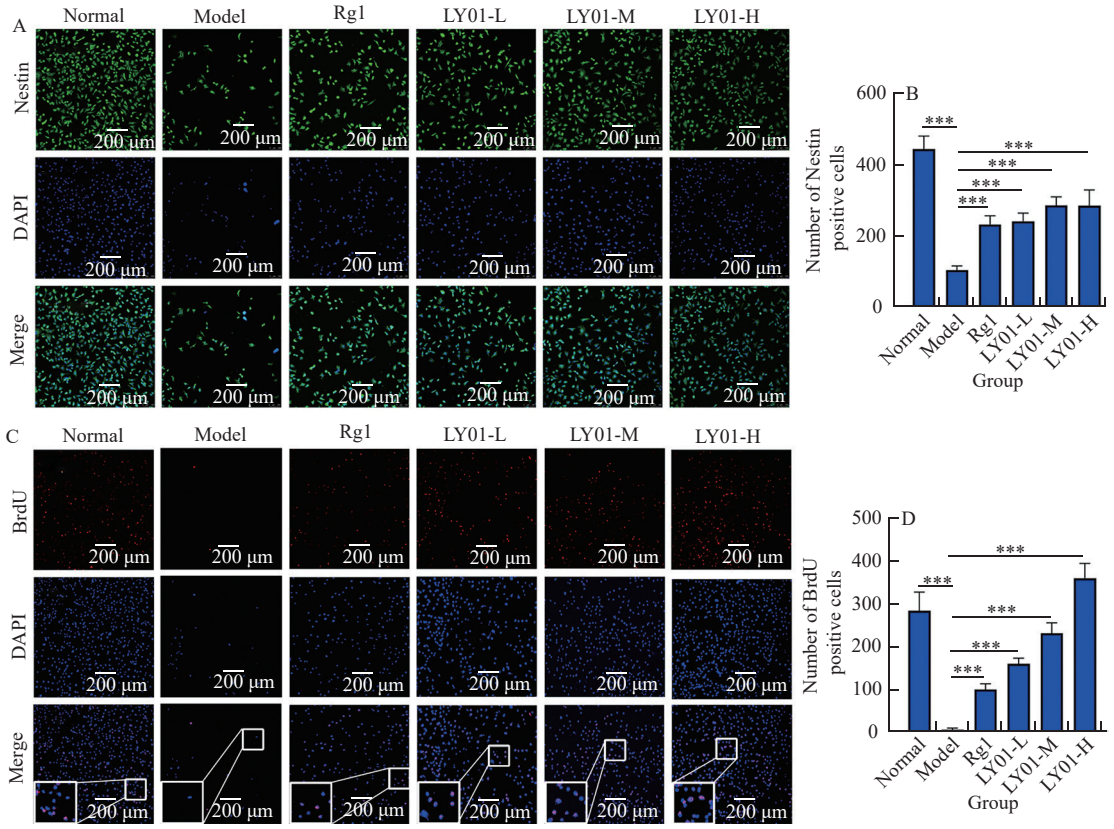

Fig. 8 LY01 promotes proliferation of C17.2 mouse NSCs. (A) Nestin immunofluorescence results. (B) Nestin positive cell count. (C) BrdU immunofluorescence results. (D) BrdU positive cell count. $n = 4$.

3.8 LY01 has the potential to activate the Wnt/β-catenin signaling pathway in C17.2 mouse NSCs

The qPCR results showed that the mRNA expressions of *Wnt3a* (Fig. 9A), *β-catenin* (Fig. 9C), and *cyclinD1* (Fig. 9D) in the model group were lower than those in the normal group (*Wnt3a*: $P < 0.05$, *β-catenin*: $P < 0.01$, *cyclinD1*: $P < 0.01$). The mRNA expression of *GSK-3β* in the model group was higher than that in the normal group ($P < 0.01$) (Fig. 9B). This indicated that oxidative damage promotes *GSK-3β* phosphorylation, reduces the production of *Wnt3a*, *β-catenin*, and *cyclinD1*; and inhibits the Wnt/β-catenin signaling pathway. In contrast, the mRNA expression of *Wnt3a* (Fig. 9A), *β-catenin* (Fig. 9C), and *cyclinD1* (Fig. 9D) was significantly higher ($P < 0.05$), and *GSK-3β* was significantly lower ($P < 0.05$), in the Rg1 and LY01 groups administered at each dose than in the model group. This indicated that the Rg1 and LY01 groups administered at each dose the drug groups had the potential to activate the Wnt/β-catenin signaling pathway in C17.2 mouse NSCs.

The WB results showed that the protein expression of Wnt3a (Fig. 9G), β-catenin (Fig. 9F), and cyclinD1 (Fig. 9H) in the model group was lower than that in the normal group ($P < 0.001$). This indicated that oxidative damage reduces the production of Wnt3a, β-catenin, and cyclinD1 and inhibits the Wnt/β-catenin signaling pathway. In contrast, the protein expression of Wnt3a (Fig. 9G), β-catenin (Fig. 9F), and cyclinD1 (Fig. 9H) was significantly higher in the Rg1 and LY01 administration groups at each dose than that in the model group ($P < 0.01$). This indicated that the Rg1 and LY01 groups administered at each dose had the potential to activate the Wnt/β-catenin signaling pathway in C17.2 mouse NSCs.

4. Discussion

NSCs proliferation is influenced by factors such as the extracellular microenvironment and intracellular signaling. In recent years, some signaling pathways that specifically affect the proliferation of NSCs have been gradually identified, including the Wnt, Notch, and Shh signaling pathways[33-34]. In particular, the Wnt signaling pathway plays a vital role in the proliferation, differentiation, and migration of NSCs. It has been classified into three pathways based on the pattern of signal transduction: the canonical Wnt/β-catenin signaling pathway activates specific genes in the nucleus; the Wnt-PCP signaling pathway regulates cytoskeletal rearrangement; the Wnt-Ca^{2+} signaling pathway stimulates the release of intracellular calcium ions[35]. The Wnt/β-catenin signaling pathway widely distributed in the brain plays an essential role in the development and maturation of the central nervous system. It is one of the critical signaling pathways regulating the proliferation of NSCs[36]. When the Wnt protein is absent, the Wnt/β-catenin pathway is inhibited. Intracellular axin, antigen-presenting cells (APC), and two kinases—GSK-3 and casein kinase type I (CK1)—form a disruption complex, which in turn mediates the phosphorylation of β-catenin. Phosphorylated β-catenin is subsequently recognized and degraded by the ubiquitin-mediated proteasome disrupting the Wnt/β-catenin pathway. The Wnt/β-catenin pathway is activated when Wnt proteins are present, and Wnt binds to the cell surface receptor frizzled (Fz) and the membrane co-receptor low-density lipoprotein receptor-related protein 5/6 (LRP5/6). This further allows dishevelled (Dvl) to accumulate near the cell membrane and bind to axin, disrupting the formation of the APC/axin/GSK-3/CK1 complex, thereby inhibiting their mediation of β-catenin phosphorylation and stabilization of β-catenin[35,37-38]. β-Catenin enters the nucleus and binds to the T-cell factor 1/Lymphoid-enhancer binding factor 1 (TCF1/LEF1) of the transcription factor family, causing transcription of the cell cycle factor cyclinD1, thus promoting the onset of NSC proliferation[39]. Therefore, induction of canonical Wnt/β-catenin signaling may be a promising approach to treating neurodegenerative diseases.

Studies have shown reduced neurogenesis in neurodegenerative disorders such as Parkinson's disease and AD[40]. Inducing nerve regeneration can reduce the occurrence of neurodegenerative diseases and

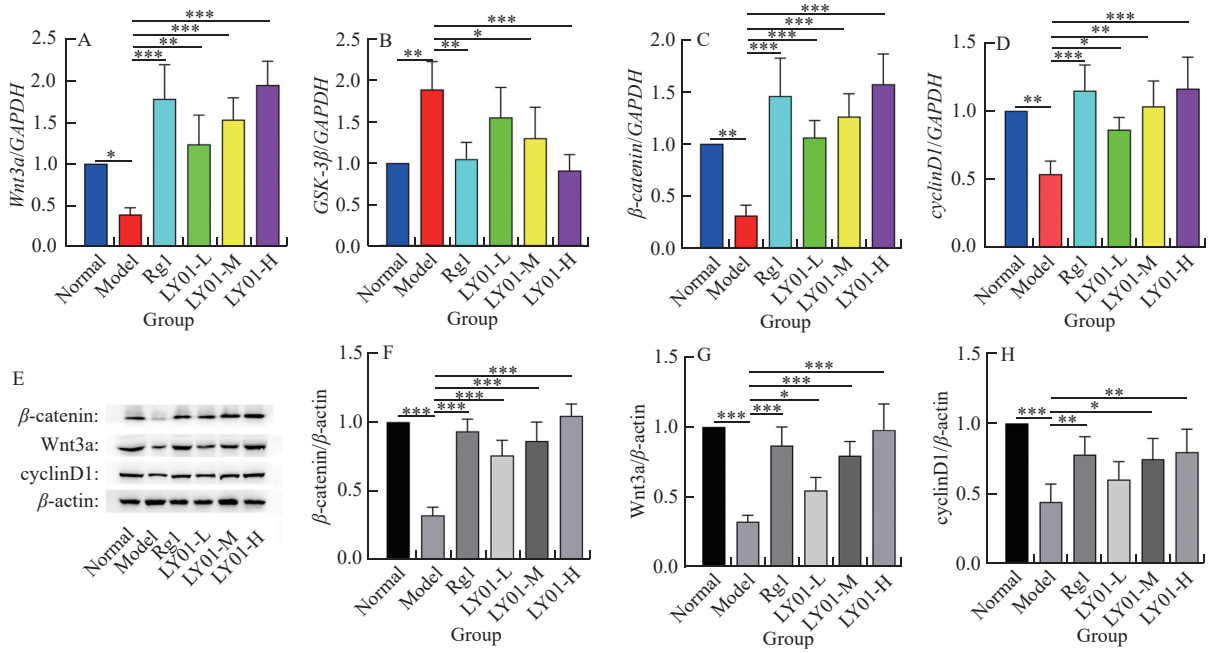

Fig. 9 LY01 promotes activation of the Wnt/β-catenin signaling pathway in C17.2 mouse NSCs. (A) Relative mRNA expression of *Wnt3a*. (B) Relative mRNA expression of *GSK-3β*. (C) Relative mRNA expression of *β-catenin*. (D) Relative mRNA expression of *cyclinD1*. (E) Protein expression of β-catenin, Wnt3a, and CyclinD1. (F) Relative protein expression of β-catenin. (G) Relative protein expression of Wnt3a. (H) Relative protein expression of cyclinD1. $n = 4$.

slow down the progression of the disease. In this study, we found that neurogenesis was reduced in 5×FAD mice under Aβ toxic injury, as evidenced by abnormal hippocampal tissue and neurons, significantly reduced proliferation of NSCs, and abnormally reduced neuronal generation in mice. LY01 treatment significantly improved cognitive impairment in 5×FAD mice, increased learning ability and memory capacity in 5×FAD mice, improved hippocampal tissue structure and neuronal morphology, and promoted the proliferation of NSCs and new neuronal generation. In *in vitro* experiments, oxidative damage also led to a significant decrease in the proliferation of NSCs in C17.2 mice. LY01 improved the cell viability and cell morphology of NSCs in C17.2 mice after hydrogen peroxide damage, as well as increasing nestin and BrdU content to promote their proliferation. In the experimental design of this study, the low-dose LY01 group did not show a significant therapeutic effect. An increase in the overall administered dose of LY01 may result in more significant efficacy.

To better research the mechanism of LY01 for AD, we investigated the Wnt pathway because it is involved in the proliferation of NSCs and is closely associated with AD risk factors[41]. Aβ toxicity leads to down-regulation of the Wnt/*β*-catenin pathway and thus up-regulation of GSK-3β, leading to neuro-tangle pathology with tau hyperphosphorylation[42]; this is identical to our findings in 5×FAD mice. Stereotaxic injection of lentiviral vectors expressing Wnt-3a or a mutant Wnt-1 that blocks the activation of the Wnt signaling cascade showed that inhibition of this pathway decreases neurogenesis, whereas stimulating the canonical Wnt pathway induces a strong increase in adult hippocampal neurogenesis[41]. LY01 upregulated Wnt3a and increased proliferation and neuronal production in the NSCs of 5×FAD mice. Progerin-1 (PS-1) is associated with AD, and the *β*-linked protein was found to be reduced in the brains of AD patients carrying a genetic mutation in PS-1[43-44]. Similarly, in 5×FAD mice, we found reduced expression of the *β*-linked protein, whereas gene and protein expression of the *β*-linked protein was significantly increased in the hippocampal tissue of 5×FAD mice after LY01 treatment. Additionally, the phosphorylation of tau antagonizes apoptosis by preventing the phosphorylation and subsequent degradation of *β*-catenin[41]. *cyclinD1*, a downstream proliferation gene of the Wnt/*β*-catenin signaling pathway, is a marker of cell cycle progression from the G1 to the S phase. It promotes cell division and proliferation by binding and activating cyclin-dependent kinases (CDKs) to bring cells into the S phase[30]. We found that LY01 upregulated cyclinD1, which may be critical in promoting proliferation and neonatal neuron generation in NSCs of 5×FAD mice. In vitro experiments verified that LY01 still has the same effect under oxidative damage. The study preliminarily explored whether LY01 has the potential to activate the Wnt/*β*-catenin signaling pathway. However, it lacks direct experimental evidence to prove the relationship between each phenotype and the Wnt/*β*-catenin signaling pathway and other pathways. Thus, the precise mechanism of LY01 must be further verified and investigated.

LY01 is an isoflavonoid with diverse bioactivities. Previous studies have reported that isoflavonoid exposure could reduce the risk of allergic reactions and chronic nasal inflammations by alleviating antioxidant damage[45-46]. Isoflavonoid can also increase nasal and oral microbial diversity and abundance of protective microbial taxa[47]. Additionally, isoflavones can modulate hepatic fructose production through the inhibition of aldose reductase and reduce stem cell steatosis, which, in turn, mitigates the development of steatohepatitis[48-49]. Therefore, LY01 likely also has a protective role against adverse health conditions.

5. Conclusions

The study indicated the ability of LY01, found in the edible fruits of *S. alopecuroides* L., to promote NSC proliferation and new neurons, thus repairing damaged neurons to encourage recovery of brain function. This correlates with the potential of LY01 to activate the Wnt/*β*-catenin signaling pathway (Fig. 10). The study has provided new ideas and alternative drugs for AD prevention and treatment, as well as a new direction in food health care.

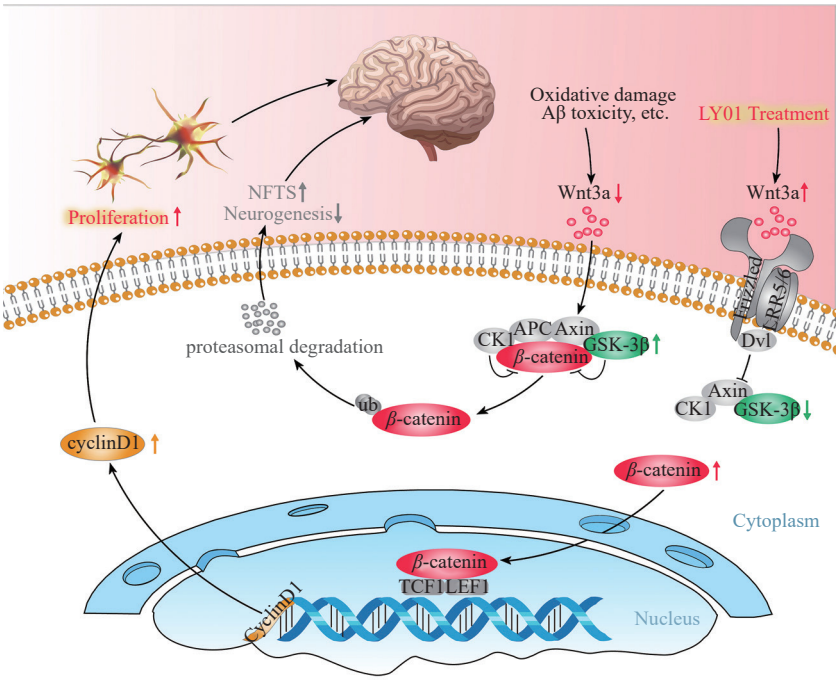

Fig. 10 Schematic diagram of LY01 acting on Wnt/*β*-catenin signaling pathway.

Conflict of interest

The authors declare that the research was conducted in the absence of any commercial or financial relationships that could be construed as a potential conflict of interest.

Acknowledgements

This work was supported by the National Nature Science Foundation of China (82174085) and Natural Science Foundation of Inner Mongolia Autonomous Region (2019MS08032).

References

[1] C. Ballard, S. Gauthier, A. Corbett, et al., Alzheimer's disease, Lancet 377 (2011) 1019-1031. https://doi.org/10.1016/S0140-6736(20)32205-4.

[2] C. Laurent, L. Buée, D. Blum, Tau and neuroinflammation: what impact for Alzheimer's disease and tauopathies? Biomed J. 41(1) (2018) 21-33. https://doi.org/10.1016/j.bj.2018.01.003.

[3] S.B. Arredondo, D. Valenzuela-Bezanilla, M.D. Mardones, et al., Role of Wnt signaling in adult hippocampal neurogenesis in health and disease, Front. Cell Dev. Biol. 8 (2020) 860. https://doi.org/10.3389/fcell.2020.00860.

[4] L.B. Ngwenya, S. Mazumder, Z.R. Porter, et al., Implantation of neuronal stem cells enhances object recognition without increasing neurogenesis after lateral fluid percussion injury in mice, Stem Cells Int. 2018 (2018) 1-11. https://doi.org/10.1155/2018/4209821.

[5] C.A. Blaiss, T.S. Yu, G. Zhang, et al., Temporally specified genetic ablation of neurogenesis impairs cognitive recovery after traumatic brain injury, J. Neurosci. 31(13) (2011) 4906-4916. https://doi.org/10.1523/JNEUROSCI.5265-10.2011.

[6] J.S. Barbosa, R. Sanchez-Gonzalez, R. di Giaimo, et al., Live imaging of adult neural stem cell behavior in the intact and injured zebrafish brain, Neurodevelopment Science 348 (2015) 789-793. https://doi.org/10.1126/science.aaa2729.

[7] B.N. Dugger, D.W. Dickson, Pathology of neurodegenerative diseases, Cold Spring Harb. Perspect. Biol. 9(7) (2017) a028035. https://doi.org/10.1101/cshperspect.a028035.

[8] X.W. Li, Y.Y. Lu, S.Y. Zhang, et al., Mechanism of neural regeneration induced by natural product LY01 in the 5×FAD mouse model of Alzheimer's disease, Front. Pharmacol. 13 (2022) 926123. https://doi.org/10.3389/fphar.2022.926123.

[9] T. Sun, L. Chen, R. Liu, et al., *Sophora alopecuroides* alleviates neuroinflammation and oxidative damage of Parkinson's disease *in vitro* and *in vivo*, Am. J. Chin. Med. 51(2) (2023) 309-328. https://doi.org/10.1142/S0192415X23500167.

[10] S. Khan, K.H. Barve, M.S. Kumar, Recent advancements in pathogenesis, diagnostics and treatment of Alzheimer's disease, Curr. Neuropharmacol. 18(11) (2020) 1106-1125. https://doi.org/10.2174/1570159X18666200528142429.

[11] S.H. Barage, K.D. Sonawane, Amyloid cascade hypothesis: pathogenesis and therapeutic strategies in Alzheimer's disease, Neuropeptides 52 (2015) 1-18. https://doi.org/10.1016/j.npep.2015.06.008.

[12] V. Calsolaro, P. Edison, Neuroinflammation in Alzheimer's disease: current evidence and future directions, Alzheimers Dement. 12(6) (2016) 719-32. https://doi.org/10.1016/j.jalz.2016.02.010.

[13] Z. Chen, C. Zhong, Oxidative stress in Alzheimer's disease, Neurosci. Bull. 30(2) (2014) 271-281. https://doi.org/10.1007/s12264-013-1423-y.

[14] H. Oakley, S.L. Cole, S. Logan, et al., Intraneuronal *β*-amyloid aggregates, neurodegeneration, and neuron loss in transgenic mice with five familial Alzheimer's disease mutations: potential factors in amyloid plaque formation, J. Neurosci. 26(40) (2006) 10129-10140. https://doi.org/10.1523/JNEUROSCI.1202-06.2006.

[15] H.Y. Liang, P.P. Zhang, X.L. Zhang, et al., Preclinical systematic review of ginsenoside Rg1 for cognitive impairment in Alzheimer's disease, Aging (Albany NY). 13(5) (2021) 7549-7569. https://doi.org/10.18632/aging.202619.

[16] J.J. Wu, Y. Yang, Y. Wan, et al., New insights into the role and mechanisms of ginsenoside Rg1 in the management of Alzheimer's disease, Biomed. Pharmacother. 152 (2022) 113207. https://doi.org/10.1016/j.biopha.2022.113207.

[17] S.J. Yang, J.J. Wang, P. Cheng, et al., Ginsenoside Rg1 in neurological diseases: from bench to bedside, Acta. Pharmacol. Sin. 44(5) (2023) 913-930. https://doi.org/10.1038/s41401-022-01022-1.

[18] H. Xiao, H. Li, H. Song, et al., Shenzao Jiannao oral liquid, an herbal formula, ameliorates cognitive impairments by rescuing neuronal death and triggering endogenous neurogenesis in AD-like mice induced by a combination of Aβ42 and scopolamine, J. Ethnopharmacol. 259 (2020) 112957. https://doi.org/10.1016/j.jep.2020.112957.

[19] C.D. Barnhart, D. Yang, P.J. Lein, Using the Morris water maze to assess spatial learning and memory in weanling mice, PLoS ONE 10(4) (2015) e0124521. https://doi.org/10.1371/journal.pone.0124521.

[20] A.L. Dinel, C. Lucas, D. Guillemet, et al., Chronic Supplementation with a mix of *Salvia officinalis* and *Salvia lavandulaefolia* improves Morris water maze learning in normal adult C57Bl/6J mice, Nutrients 12(6) (2020) 1777. https://doi.org/10.3390/nu12061777.

[21] S. Li, Y. Li, W. Sun, et al., Sanwei DouKou decoction ameliorate Alzheimer disease by increasing endogenous neural stem cells proliferation through the Wnt/*β*-catenin signaling pathway, J. Ethnopharmacol. 309 (2023) 116364. https://doi.org/10.1016/j.jep.2023.116364.

[22] M. Ramezani, N. Darbandi, F. Khodagholi, et al., Myricetin protects hippocampal CA3 pyramidal neurons and improves learning and memory impairments in rats with Alzheimer's disease, Neural. Regen. Res. 11(12) (2016) 1976-1980. https://doi.org/10.4103/1673-5374.197141.

[23] B. Wang, S. Jedlicka, X. Cheng, Maintenance and neuronal cell differentiation of neural stem cells C17.2 correlated to medium availability sets design criteria in microfluidic systems, PLoS ONE 9(10) (2014) e109815. https://doi.org/10.1371/journal.pone.0109815.

[24] W. Wang, T. Yan, X. Guo, et al., KAP1 phosphorylation promotes the survival of neural stem cells after ischemia/reperfusion by maintaining the stability of PCNA, Stem Cell Res. Ther. 13(1)(2022) 290. https://doi.org/10.1186/s13287-022-02962-5.

[25] S. Chavoshinezhad, H. Mohseni Kouchesfahani, A. Ahmadiani, et al., Interferon beta ameliorates cognitive dysfunction in a rat model of Alzheimer's disease: modulation of hippocampal neurogenesis and apoptosis as underlying mechanism, Prog. Neuropsychopharmacol. Biol. Psychiatry 94 (2019) 109661. https://doi.org/10.1016/j.pnpbp.2019.109661.

[26] W. Mao, X. Yi, J. Qin, et al., CXCL12 promotes proliferation of radial glia like cells after traumatic brain injury in rats, Cytokine 125 (2020) 154771. https://doi.org/10.1016/j.cyto.2019.154771.

[27] Y. Sun, J. Huang, Y. Chen, et al., Direct inhibition of Keap1-Nrf2 protein-protein interaction as a potential therapeutic strategy for Alzheimer's disease, Bioorg. Chem. 103 (2020) 104172. https://doi.org/10.1016/j.bioorg.2020.104172.

[28] X. Zhang, Y. Hei, W. Bai, et al., Toll-Like receptor 2 attenuates traumatic brain injury-induced neural stem cell proliferation in dentate gyrus of rats, Neural. Plast. 2020 (2020) 1-10. https://doi.org/10.1155/2020/9814978.

[29] S.K. Tiwari, B. Seth, S. Agarwal, et al., Ethosuximide induces hippocampal neurogenesis and reverses cognitive deficits in an amyloid-β toxin-induced Alzheimer rat model *via* the phosphatidylinositol 3-kinase (PI3K)/Akt/Wnt/*β*-catenin pathway, J. Biol. Chem. 290(47) (2015) 28540-28558. https://doi.org/10.1074/jbc.M115.652586.

[30] S.R. Li, Y.J. Song, R. Deng, et al., *Mallotus oblongifolius* extracts ameliorate ischemic nerve damage by increasing endogenous neural stem cell proliferation through the Wnt/*β*-catenin signaling pathway, Food Funct. 11(1) (2020) 1027-1036. https://doi.org/10.1039/C9FO01790A.

[31] H.H. Xiao, M.B. Zhang, J.T. Xu, et al., Icarisid II promotes proliferation and neuronal differentiation of neural stem cells *via* activating Wnt/*β*-catenin signaling pathway, Phytother. Res. 35(5) (2021) 2773-2784. https://doi.org/10.1002/ptr.7022.

[32] X.K. Tong, J. Royea, E. Hamel, Simvastatin rescues memory and granule cell maturation through the Wnt/*β*-catenin signaling pathway in a mouse model of Alzheimer's disease, Cell Death Dis. 13(4) (2022) 325. https://doi.org/10.1038/s41419-022-04784-y.

[33] J. Li, Y. Han, M. Li, et al., Curcumin promotes proliferation of adult neural stem cells and the birth of neurons in Alzheimer's disease mice *via* Notch

signaling pathway, Cell. Reprogram. 21(3) (2019) 152-161. https://doi.org/10.1089/cell.2018.0027.

[34] Y. Xiao, D.T. Thoresen, J.S. Williams, et al., Neural hedgehog signaling maintains stem cell renewal in the sensory touch dome epithelium, Proc. Natl. Acad. Sci. 112(23) (2015) 7195-7200. https://doi.org/10.1073/pnas.1504177112.

[35] Y. Komiya, R. Habas, Wnt signal transduction pathways, Organogenesis 4(2) (2008) 68-75. https://doi.org/10.4161/org.4.2.5851.

[36] M. Kléber, L. Sommer, Wnt signaling and the regulation of stem cell function, Curr. Opin. Cell Biol. 16(6) (2004) 681-687. https://doi.org/10.1016/j.ceb.2004.08.006.

[37] S.P. Acebron, E. Karaulanov, B.S. Berger, et al., Mitotic Wnt signaling promotes protein stabilization and regulates cell size, Mol. Cell. 54(4) (2014) 663-674. https://doi.org/10.1016/j.molcel.2014.04.014.

[38] J. Bilic, Y.L. Huang, G. Davidson, et al., Wnt induces LRP6 signalosomes and promotes dishevelled-dependent LRP6 phosphorylation, Science 316 (2007) 1619-1622. https://doi.org/10.1126/science.1137065.

[39] W.M. Zhang, Z.R. Zhang, X.T. Yang, et al., Overexpression of miR-21 promotes neural stem cell proliferation and neural differentiation *via* the Wnt/*β*-catenin signaling pathway *in vitro*, Mol. Med. Rep. 17(1) (2018) 330-335. https://doi.org/10.3892/mmr.2017.7856.

[40] B. Steiner, S. Wolf, G. Kempermann, Adult neurogenesis and neurodegenerative disease, Regen. Med. 1(1) (2006) 15-28. https://doi.org/10.2217/17460751.1.1.15.

[41] N.C. Inestrosa, L. Varela-Nallar, Wnt signaling in the nervous system and in Alzheimer's disease, J. Mol. Cell Biol. 6(1) (2014) 64-74. https://doi.org/10.1093/jmcb/mjt051.

[42] R.A. Boonen, P. van Tijn, D. Zivkovic, Wnt signaling in Alzheimer's disease: up or down, that is the question, Ageing Res. Rev. 8(2) (2009) 71-82. https://doi.org/10.1016/j.arr.2008.11.003.

[43] Z. Zhang, H. Hartmann, V.M. Do, et al., Destabilization of *β*-catenin by mutations in presenilin-1 potentiates neuronal apoptosis, Nature 395(6703) (1998) 698-702. https://doi.org/10.1038/27208.

[44] D.C. Lie, S.A. Colamarino, H.J. Song, et al., Wnt signalling regulates adult hippocampal neurogenesis, Nature 437 (2005) 1370-1375. https://doi.org/10.1038/nature04108.

[45] Y. Sun, M. Zhang, Z. Ou, et al. Indoor microbiome, microbial and plant metabolites, chemical compounds, and asthma symptoms in junior high school students: a multicentre association study in Malaysia, Eur. Respir. J. 60(5) (2022) 2200260. https://doi.org/10.1183/13993003.00260-2022.

[46] Y. Sun, H. Tang, S. Du, et al. Indoor metabolites and chemicals outperform microbiome in classifying childhood asthma and allergic rhinitis, Eco Environ. Health. 2(4) (2023) 208-218. https://doi.org/10.1016/j.eehl.2023.08.001.

[47] M. Zhang, H. Tang, Y. Yuan, et al. The role of indoor microbiome and metabolites in shaping children's nasal and oral microbiota: a pilot multi-omic analysis, Metabolites 13(10) (2023) 1040. https://doi.org/10.3390/metabo13101040.

[48] C. Veeresham, A. Rama Rao, K. Asres, Aldose reductase inhibitors of plant origin, Phytother. Res. 28(3) (2014) 317-333. https://doi.org/10.1002/ptr.5000.

[49] M.A. Lanaspa, T. Ishimoto, N. Li, et al., Endogenous fructose production and metabolism in the liver contributes to the development of metabolic syndrome, Nat. Commun. 4(1) (2013) 2434. https://doi.org/10.1038/ncomms3434.